

05.3;13.1;14.1;15.2

Production of titanium and gold particles by laser ablation of thin films in water

© V.S. Zhigarkov¹, E.V. Ivanovskaya², K.O. Aiyzyhy³, A.V. Ovcharov⁴

¹ Institute of Photon Technologies, Federal Scientific Research Center „Crystallography and Photonics“, Russian Academy of Sciences, Troitsk, Moscow, Russia

² Mendeleev University of Chemical Technology, Moscow, Russia

³ Prokhorov Institute of General Physics, Russian Academy of Sciences, Moscow, Russia

⁴ National Research Centre „Kurchatov Institute,“, Moscow, Russia

E-mail: vzhigarkov@gmail.com

Received June 9, 2023

Revised October 2, 2023

Accepted October 2, 2023

Suspensions of metal particles based on titanium and gold were obtained by pulsed laser ablation of thin metal films on glass substrates in contact with water. The particles were characterized by scanning electron microscopy and dynamic light scattering. It is shown that the particles are polydisperse. The particle size varies depending on the of the laser energy. For particles based on titanium, two fractions are distinguished with sizes of 74–180 nm and 510–635 nm. In the case of gold nanoparticles, their size does not exceed 100 nm. However, at the maximum energy of the laser pulse a fraction with a size of 416 ± 28 nm appears. The values of the zeta potentials and the concentration of particle solutions are given.

Keywords: pulsed laser ablation, thin films, titanium and gold nanoparticles, dynamic light scattering, scanning electron microscopy.

DOI: 10.61011/TPL.2023.11.57204.19649

The study of properties and specific features of nanoparticles and their ensembles is of a great academic and practical interest. The properties and characteristics of particles depend on the method of their production. Pulsed laser ablation (PLA) of bulk metal targets and thin films immersed in liquid is one of the methods of this kind. The potential to produce high-purity particles is among the advantages of PLA. In addition, this method is multipurpose in the sense that it allows one to synthesize particles with various properties in vast numbers. Synthesized nanoparticles are used widely at present for biological and medical purposes. This is motivated, on the one hand, by their unique optical properties that enable the use of nanoparticles as optical sensors for sample detection [1]. On the other hand, they have a large specific surface area and an elevated reactivity that allow them to penetrate through biological membranes. One may alter the toxic effect of nanoparticles on cells by adjusting the nanoparticle concentration and produce, e.g., antimicrobial drugs [2]. Donor transparent glasses with a metal absorbing layer based on gold [3,4] or titanium [4] are used in the known cell printing technique that relies on laser-induced forward transfer of matter (LIFT). However, pulsed irradiation results in ejection of gold and titanium oxide particles as waste along with a droplet that contains live cells and biomolecules [4].

In the case of titanium oxide, an important part is played by its crystalline phase, which also needs to be taken into account in the design of biomaterials based on this oxide [5]. A modern man is subjected to a constant influence of TiO₂ particles coming from food items and hygiene products

where these particles are used as a dye [6]. The size of particles and the scenario of exposure specify their reactivity in cells of biological organisms [7]. For example, TiO₂ particles less than 100 nm in size are readily internalized by bone cells and elicit oxidative stress and cell death [5]. At the same time, submicrometer TiO₂ particles are far less toxic [8]. Thus, further research into this material is relevant and important in many fields.

The demand for gold nanoparticles in various domains is spurred by their unique properties: a large specific surface area and widely varying surface characteristics. This has inspired the design of nanoelectronic chips and enabled the progress in ecological and biomedical applications [9]. They are currently being studied extensively in the context of practical applications in medicine. Gold nanoparticles are used as cellular and biomolecular markers in microscopy and diagnostics and as drug carriers to raise the efficiency of treatment and lower the side effects of various therapy techniques [9,10].

The aim of the present study is to prepare aqueous solutions of titanium- and gold-based particles by PLA of thin films of glass substrates. The concentrations of obtained solutions, size distributions, and the values of ζ -potential, which characterizes the reactivity of particles, are reported.

A laser system with a nanosecond laser was used to synthesize nanoparticles. The diagram of the experiment is shown in Fig. 1. An YLPM-1-4x200-20-20 pulsed fiber laser (OOO NTO „IRE-Polyus,“ Russia) with beam propagation parameter $M^2 < 1.5$ was the radiation source. The radiation wavelength was 1064 nm, and the pulse

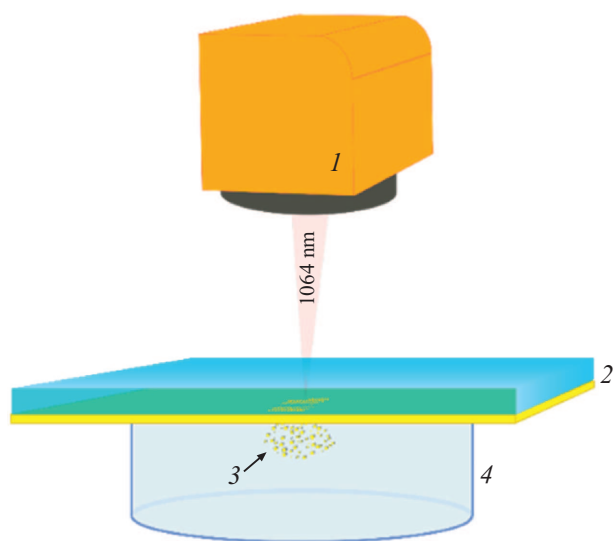


Figure 1. General diagram of the experiment. 1 — Galvanic scanning head with a long-focus objective, 2 — donor glass substrate with a metal film, 3 — metal nanoparticles, and 4 — cuvette with milli-Q water.

width was 8 ns. An LscanH-10-1064 (AtekoTM, Russia) double-mirror galvanic scanning head fitted with an F-theta SL-1064-110-160 objective (Ronar-Smith, Singapore) with a focal distance of 160 mm, which provides a laser beam diameter at focus of $30 \pm 2 \mu\text{m}$, was used to control the process of irradiation. The pulse energy was calibrated with the use of a QE8SP-MT-INT (Gentec-EO, Quebec City, QC, Canada) pyroelectric detector. The experimental energy range was 16–45 μJ .

Titanium and gold films deposited onto specimen glasses $26 \times 76 \times 1 \text{ mm}$ in size (Menzel Glaser, Germany) by magnetron sputtering were used as targets. The thickness of metal films was 50 nm.

Metal films on donor substrates were ablated in milli-Q water. The volume of water in a cuvette was 3 ml. Laser processing was performed by sequential pulses in the form of 150×150 matrices. The distance between matrix elements was $50 \mu\text{m}$, and the overall number of pulses was 45 000.

Dynamic light scattering (DLS) and a Zetasizer Ultra (Malvern Panalytical) analyzer were used to determine the size and measure the concentration and the ζ -potential of synthesized particles. The obtained nanoparticles and microstructures were examined with a Helios Nanolab 600i scanning electron-ion microscope (FEI, United States).

The scanning electron microscope (SEM) images in Fig. 2 reveal polydisperse systems with a broad particle size distribution. This becomes clearly evident when one examines Fig. 2, *a* that presents the data for particles based on titanium(IV) oxide [4]. Generally speaking, titanium dioxide is used in the production of sensors, photoelectrodes, solar cells, and photocatalysts for decomposition of a wide range of organic and inorganic substances [11]. As was demonstrated earlier, the primary forms of titanium dioxide produced as a result of laser ablation are rutile and anatase [12]. These compounds are highly catalytically and biologically active. Note that particles seen in both SEM images have predominantly spherical shapes and are prone to aggregation.

Standard measurements of the hydrodynamic diameter, the surface charge, and the concentration of particles in a solution were performed in order to characterize the obtained particles in more detail. The data on dynamic light

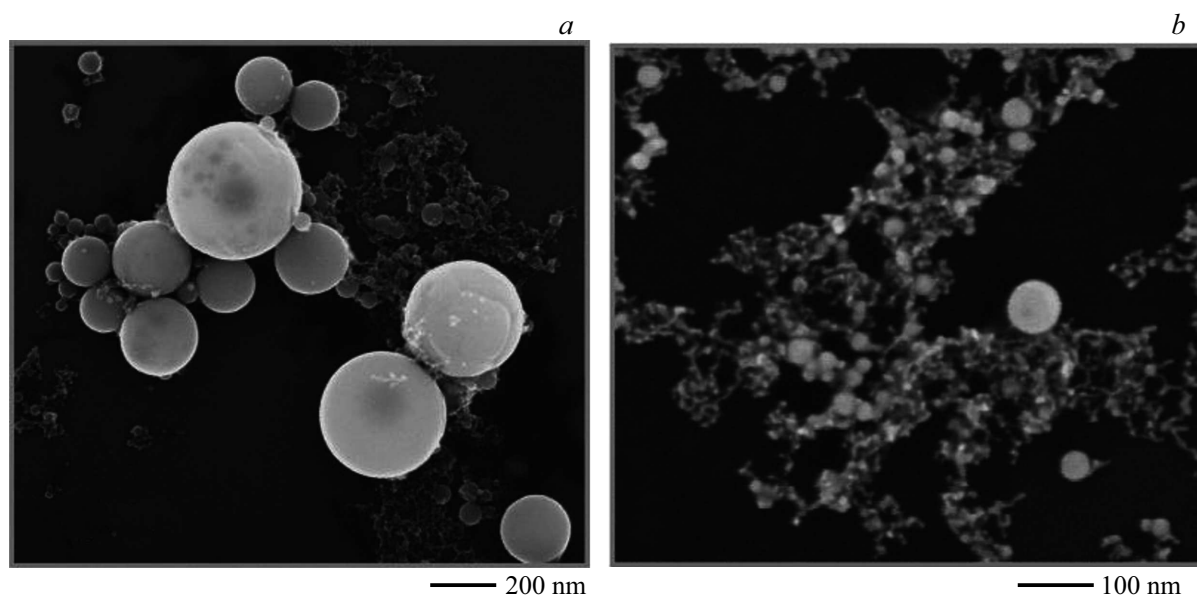


Figure 2. SEM images of metal particles on a silicon substrate. *a* — Titanium-based particles prepared by processing a film at an energy of 16 μJ ; *b* — gold nanoparticles fabricated by processing a film at an energy of 35 μJ .

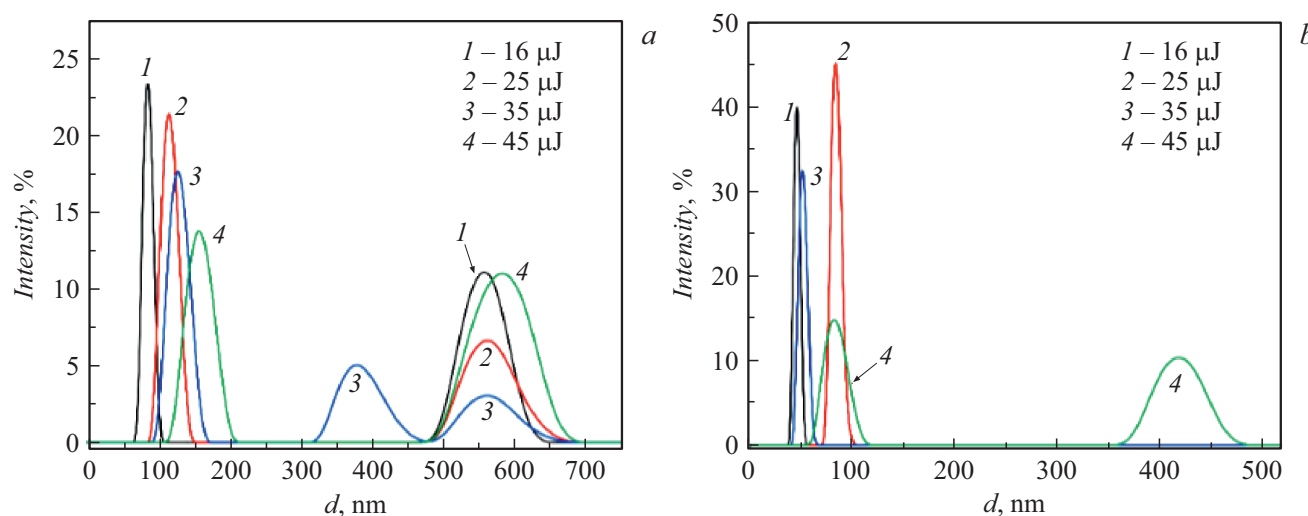


Figure 3. Distributions over hydrodynamic diameters of metal particles in water obtained by DLS. *a* — Titanium particles; *b* — gold particles.

Characteristics determined via dynamic light scattering

Metal film	Pulse energy, μJ	Mean hydrodynamic diameter, nm	Concentration, particles/ml	ξ -potential, mV
Titanium	16	82 ± 8 550 ± 40	$6.80 \cdot 10^8$ $3.23 \cdot 10^4$	-2.3
	25	110 ± 20 560 ± 40	$1.63 \cdot 10^8$ $3.11 \cdot 10^4$	-0.7
	35	130 ± 20 370 ± 30 560 ± 40	$6.93 \cdot 10^7$ $1.37 \cdot 10^5$ $1.81 \cdot 10^4$	-17.3
	45	150 ± 30 580 ± 60	$2.53 \cdot 10^7$ $3.45 \cdot 10^4$	-22.1
Gold	16	46 ± 4	$2.34 \cdot 10^{11}$	-5.4
	25	84 ± 7	$6.58 \cdot 10^{10}$	-22.4
	35	52 ± 6	$1.22 \cdot 10^{12}$	-24.2
	45	80 ± 10 420 ± 30	$4.19 \cdot 10^{10}$ $3.03 \cdot 10^7$	-32.4

scattering in Fig. 3 were processed and presented in tabular form. It should be noted that coarse fractions in SEM images are prone to rapid sedimentation; therefore, they could not be identified unambiguously in DLS experiments.

Figure 3 and the table present the results obtained by DLS. At least 2-3 fractions of different sizes formed in all experiments with particles based on titanium(IV) oxide (Fig. 3, *a*). It is common knowledge that the size of forming nanoparticles is governed by the thermal conductivity of a target and the radiation energy density [13,14]. In addition, the distribution function is affected by the process of interaction between nanoparticles and the laser beam, which may lead to particle fragmentation due to melting and the development of hydrodynamic

instabilities at the melt–liquid vapor interface [13,14]. However, the presence of coarse particle fractions in experiments may also be attributed to the generation of submerged jets [15]. Fractions with a high concentration of 10^7 – 10^8 particles/ml and a hydrodynamic particle diameter below 200 nm were observed in each sample. Coarse particle fractions had a significantly lower concentration of 10^4 – 10^5 particles/ml. The ξ -potential of suspensions prepared at an ablation energy of 16 and 25 μJ was close to zero. It is reasonable in this case to label these particles as prone to sedimentation and coagulation. At energies of 35 and 45 μJ , the ξ -potential magnitude did not exceed 30 mV, indicating that the obtained suspension was unstable [16].

The mean hydrodynamic diameter of gold particles did not exceed 100 nm (Fig. 3, *b*) at all the studied energies except the maximum one. Their concentration (10^{10} – 10^{12} particles/ml) was several orders of magnitude higher than the one of titanium-based particles produced under the same process conditions. This is attributable to the specific features of a gold film: its weak adhesion and impact separation from the substrate surface as a result of pulsed laser irradiation [17,18]. The presence of a coarse fraction (420 ± 30 nm) produced under the maximum pulse energy ($45 \mu\text{J}$) may be attributed to the same reasons. The ξ -potential increased in magnitude as the energy grew higher. The measured ξ -potential magnitude of the disperse system was at its minimum (5.4 mV) at a pulse energy of $16 \mu\text{J}$. This is indicative of coagulation of the obtained solution [16]. At energies of 25 and $35 \mu\text{J}$, the ξ -potential magnitude did not exceed 30 mV, indicating a certain instability of the colloidal system. At $45 \mu\text{J}$, the ξ -potential magnitude exceeded 30 mV. This suggests that the colloidal solution was relatively stable and fit for long-term storage without particle sedimentation [16].

It follows from the table that the ξ -potential values of the obtained particles vary. This is attributable to the fact that these values are affected by the chemical composition of particles and their size, shape, surface functionalization, and concentration in the solution.

Thus, suspensions of particles were prepared by PLA of thin titanium and gold films in contact with water and were then examined thoroughly. The obtained results are of interest in the context of fabrication and characterization of particles with various physical and chemical properties and are relevant to practical biomedical purposes and applications.

Acknowledgments

Electron microscopy studies were carried out at the Probe and Electron Microscopy Resource Center of the National Research Center „Kurchatov Institute.“

Funding

Laser ablation experiments were supported by grant 20-14-00286 from the Russian Science Foundation, and magnetron sputtering of thin films was performed under the state assignment of the Federal Scientific Research Center „Crystallography and Photonics“ of the Russian Academy of Sciences.

Conflict of interest

The authors declare that they have no conflict of interest.

References

[1] T. Mocan, C.T. Matea, T. Pop, O. Mosteanu, A.D. Buzoianu, C. Puia, C. Iancu, L. Mocan, J. Nanobiotechnol., **15**, 25 (2017). DOI: 10.1186/s12951-017-0260-y

- [2] L. Rizzello, P.P. Pompa, Chem. Soc. Rev., **43** (5), 1501 (2014). DOI: 10.1039/C3CS60218D
- [3] L. Koch, S. Kuhn, H. Sorg, M. Gruene, S. Schlie, R. Gaebel, B. Polchow, K. Reimers, S. Stoelting, N. Ma, P.M. Vogt, G. Steinhoff, B. Chichkov, Tissue Eng. C, **16** (5), 847 (2010). DOI: 10.1089/ten.tec.2009.0397
- [4] V. Zhigarkov, I. Volchkov, V. Yusupov, B. Chichkov, Nanomaterials, **11** (10), 2584 (2021). DOI: 10.3390/nano11102584
- [5] C.B. Tovani, C.R. Ferreira, A.M.S. Simão, M. Bolean, L. Coppeta, N. Rosato, M. Bottini, P. Ciancaglini, A.P. Ramos, ACS Omega, **5** (27), 16491 (2020). DOI: 10.1021/acsomega.0c00900
- [6] A. Weir, P. Westerhoff, L. Fabricius, K. Hristovski, N. von Goetz, Environ. Sci. Technol., **46** (4), 2242 (2012). DOI: 10.1021/es204168d
- [7] J. Hou, L. Wang, C. Wang, S. Zhang, H. Liu, S. Li, X. Wang, J. Environ. Sci., **75**, 40 (2019). DOI: 10.1016/j.jes.2018.06.010
- [8] M.I. Setyawati, C.Y. Tay, S.L. Chia, S.L. Goh, W. Fang, M.J. Neo, H.C. Chong, S.M. Tan, S.C.J. Loo, K.W. Ng, J.P. Xie, C.N. Ong, N.S. Tan, D.T. Leong, Nature Commun., **4** (1), 1673 (2013). DOI: 10.1038/ncomms2655
- [9] A. Sani, C. Cao, D. Cui, Biochem. Biophys. Rep., **10** (26), 100991 (2021). DOI: 10.1016/j.bbrep.2021.100991
- [10] N. Khlebtsov, L. Dykman, Chem. Soc. Rev., **40** (3), 1647 (2011). DOI: 10.1039/C0CS00018C
- [11] N.V. Chirkunova, M.V. Dorogov, A.E. Romanov, Tech. Phys. Lett., **49** (6), 5 (2023).
- [12] A. Nath, S.S. Laha, A. Khare, Appl. Surf. Sci., **257** (7), 3118 (2011). DOI: 10.1016/j.apsusc.2010.10.126
- [13] A.V. Simakin, V.V. Voronov, N.A. Kirichenko, G.A. Shafeev, Appl. Phys. A, **79** (4-6), 1127 (2004). DOI: 10.1007/s00339-004-2660-8
- [14] P.V. Kazakevich, A.V. Simakin, V.V. Voronov, G.A. Shafeev, Appl. Surf. Sci., **252** (13), 4373 (2006). DOI: 10.1016/j.apsusc.2005.06.059
- [15] V.M. Chudnovskii, V.I. Yusupov, Tech. Phys. Lett., **46** (10), 1024 (2020). DOI: 10.1134/S1063785020100211.
- [16] B. Salopek, D. Krsić, S. Filipović, Rudarsko-Geolosko-Naftni Zbornik, **4** (1), 147 (1992). <https://hrcak.srce.hr/24757>
- [17] V.S. Zhigarkov, N.V. Minaev, V.I. Yusupov, Tech. Phys. Lett., **47**, 633 (2021). DOI: 10.1134/S1063785021060298.
- [18] V.S. Zhigarkov, N.V. Minaev, V.I. Yusupov, Quantum Electron., **50** (12), 1134 (2020). DOI: 10.1070/QEL17426.

Translated by D.Safin